We are IntechOpen,
the world's leading publisher of
Open Access books
Built by scientists, for scientists

6,900
Open access books available

185,000
International authors and editors

200M
Downloads

154
Countries delivered to

Our authors are among the

TOP 1%
most cited scientists

12.2%
Contributors from top 500 universities

CLARIVATE ANALYTICS
BOOK CITATION INDEX
INDEXED

WEB OF SCIENCE™

Selection of our books indexed in the Book Citation Index
in Web of Science™ Core Collection (BKCI)

Interested in publishing with us?
Contact book.department@intechopen.com

Numbers displayed above are based on latest data collected.
For more information visit www.intechopen.com

Inductively Coupled Telemetry in Spinal Fusion Application Using Capacitive Strain Sensors

Ji-Tzuoh Lin, Douglas Jackson, Julia Aebersold,
Kevin Walsh, John Naber and William Hnat
University of Louisville
USA

1. Introduction

Titanium or stainless steel rods are implanted to stabilize vertebrae movement during spinal fusion surgery, which allows bone grafts to fuse two or more vertebrae. Radiograph images (x-rays), computed tomography scans (CT) and magnetic resonance imaging (MRI) procedures are used to assess fusion progress and diagnose problems during patient recovery. However, the imaging techniques yield subjective results (Vamvanij et al.,1998) and as a consequence, result in unnecessary exploratory surgeries to ascertain the efficacy of the spinal fusion surgery. As the grafted bone fuses, the bending strain of the implanted rods decreases as the load is transferred to the fused vertebrae (Kanayama et al., 1997). Strain is measurable on the spinal fusion fixture, normally a stainless or titanium rod. In other words, the amount of strain is an indicator of the load applied to the rod. Therefore, it is proposed that the strain on the implant rods can be used as an alternative and non-invasive method to monitor the progress of spinal fusion (Hnat et al., 2008).

This chapter will demonstrate the realization of a telemetric strain measurement system for the spinal fusion detection as illustrated in Fig. 1. The system is composed of three major components: a sensitive strain sensor, a battery free transducer circuit that wirelessly interfaces the strain sensor, and an external interrogating reader that provides power to the implant as well as collects strain information from the transducer circuit. Research has shown that less power is consumed by a capacitive sensor than the resistive counterpart (Puers, 1993). In addition, the sensors require high sensitivity to eliminate the need for amplification that would require additional power. Therefore, the novel capacitive strain sensors are developed to meet both the power and sensitivity demand. Additional, in making the measurements a bodily-like situation, the sensor system, including the transducer circuit, is assembled on a housing (Aebersold et al., 2007) that is capable of transferring the strain from the rod to the sensor and accommodating for the size constrain. The testing loads on the rods will be provided by a material test system (MTS) with a corpectomy model fixture.

Although most strain sensors are capable of measuring axial strain due to tension and compression or their equivalents derived from bending, a sensitive bending strain sensor

that only responds to bending strain is also desirable for spinal fusion purpose. The strain sensor is expected to measure 1000 με based on an adult of 200 pounds in a corpectomy model under bending with 2 stainless spinal fusion rods (6.4 mm in diameter and 50.8 mm long) implanted (Gibson, 2002).
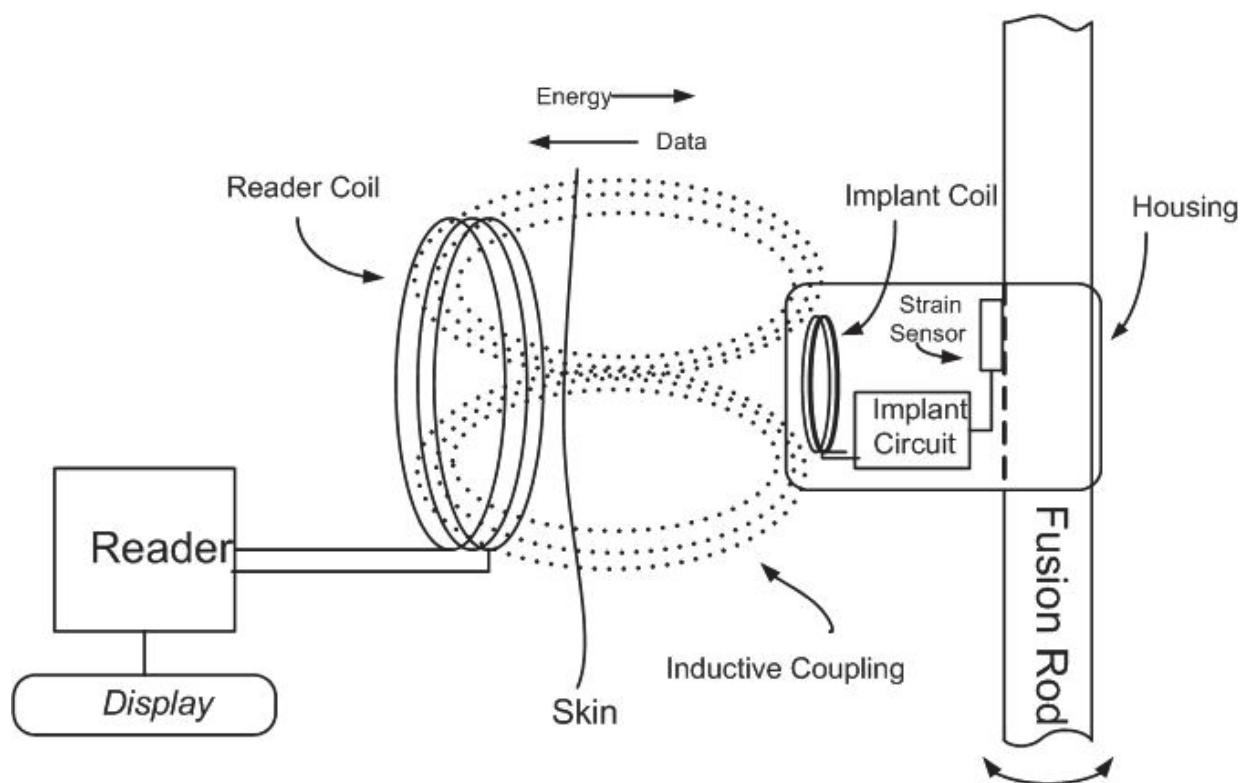

Fig. 1. A strain gauge telemetry application in spinal fusion.

MEMS capacitive sensors using wireless data transmission have been evaluated in many applications such as humidity (DeHennis & Wise, 2005; Harpster et al., 2002;), temperature (DeHennis & Wise, 2005) and pressure sensing devices (Akar et al., 2001; Chatzandroulis et al., 2000; DeHennis & Wise, 2002, 2005; Strong et al., 2002). The telemetry approach to monitor strain uses inductively coupled battery-less technology similar to the technology used in Radio Frequency IDentification (RFID) devices (Finkenzeller, 1999). Some examples of the early applications are shown in Table 1. The inductively coupled wireless system with sensing capability needs not only the working passive telemetry circuitry, but also both the sensor interface circuitry and the sensor themselves. A fully integrated implanted sensor system was realized (Chatzandroulis et al., 2000) with a capacitive pressure sensor and an application-specific integrated circuit (ASIC) chip that controls RF modulation and converts capacitance variations into frequency variations. Suster et al. developed a wireless strain detection with the transducer coil size of 3-inch coaxial to the interrogating reader (Suster et al., 2005). However, this transducer coil size is not desirable for spinal fusion implant. Research using this technique coupled with MEMS sensors has become widespread in biomedical applications. It is a promising approach for orthopedic implant sensors and the key is a highly sensitive capacitive sensor (Benzel et al., 2002).

Author, year	Chatzandroulis et al. 2000	DeHennis et al. 2002	DeHennis et al. 2005	Suster et al. 2005
Method	Backscattering	Backscatterin, C-F converter	Backscattering, C-F converter	Backscttering, C-F, F-V converter
Sensor	Capacitive pressure	Capacitive sensor	Capacitive sensor	Capacitive strain sensor
Range			4cm	1 inch
Frequency	40.68MHz	800KHz	3.18MHz	50MHz
Secondary coil			4.5mmx7.5mm	Co-axial 3 inches coils
Applications	Pressure sensor	Pressure	Pressure, humidity and temperature	Strain
Overall sensor and circuit size	450μm in diameter 2mm x 2mm	2mmx2mm sensor on chip with circuit	4.5mmx7.5mmx1mm	1000μm
Mounting	ASIC chip		On silicon	On silicon
Testing method				3-point bending
Circuit type	C/F converter	CMOS ring oscillator	Current source and relaxation oscillator	Voltage output
Number of channels	1	3 channels	3 channels	1 channel
Reader type	MC68HC705 micro-controller	Class E amplifier	Class E amplifier	
Strain/pressure range				1000 μs
Dynamic/static		Dynamic/static	Dynamic/static	Dynamic/static
Capacitance range		5pF – 33pF	0.5pF-6pF	440fF

Table 1. Some details of the inductively coupled detection systems

In the next sections, the highly sensitive MEMS bending strain sensor will be described in great detail followed by the system circuitry and the testing methods.

2. The MEMS strain sensors

This section focuses on the development and fabrication of the custom bending strain capacitive sensing element needed for the spinal fusion measurement implant (SFMI) applications. This application requires a high bending strain sensitivity with enough nominal capacitance to avoid loss due to parasitic capacitance, compatibility with an inductively powered circuit, and suitable dimensions for system packaging. The sensitive bending strain sensor is expected to be packaged in a housing container that attaches to the diameter spinal fusion rod. The distance between two vertebrae is about 25.4 mm in the lumber region, making the maximum length of the housing limited to approximately 12 mm long. Therefore, it is desirable that the sensor length be less than 10 mm. The housing is installed between two pedicle screws and needs to transfer the bending strain from the rod to the sensor as described in (Aebersold et al. 2007). The curved surface of the rod is compensated with the 2 mm thick plastic housing which conforms to the rod and is trimmed 1 mm down to provide a flat area of 2 mm x 10 mm for the sensor to mount.

Certain characteristics were primarily considered when reviewing limited examples of previous parallel plate capacitive strain sensors in the literature. The basic concept of the capacitive strain sensor features a pair of metalized parallel plates with a dielectric gap. The sensing mechanism manifests itself in varying either the area of the plate, the gap between the plates, or the dielectric medium between the plates. A number of parallel plate sensor designs with a variable air gap were analyzed in the early 90's (Procter & Strong 1992). These sensors generally exhibited low nominal capacitance and sensitivity due to the large gap. In an attempt to increase the nominal capacitance in a non-air gap design, it was demonstrated by a sensor with a parallel plate structure and a thick-film dielectric material (Arshak et al., 1994). The dielectric film between the two plates was compressed during bending, thus expanding the film in area and decreasing the thickness from the perspective of the electrodes. These changes in the film geometry lead to a high gauge factor of 75-80 with a 15-25 μm gap based on a uniform model. The capacitive gauge factor is defined by the fractional change in capacitance with respect to strain. This thick-film dielectric produced both capacitive and resistive responses to strain making this approach electrically unique, but undesirable for the SFMI application due to power consumption. In another design, more effort was involved to invoke the change in permittivity of a dielectric material resulting in a gauge factor of 3.5 to 6, with a 150 μm gap (Arshak et al., 2000). This variable permittivity approach exhibits limited sensitivity that showed no dependency on its dimension (the gauge factor is constant and only depends on the "piezocapacitive" effect). This low gauge factor approach would require additional circuitry that is not desired for this implant design.

2.1 The bending sensor theory

The mechanism of sensing pure bending on a test substrate is described in two folds: the capacitance and the strain condition imposed on the sensor, as illustrated in Fig. 2. Assuming the bending sensor is attached to a steal cantilever with length L and thickness R in an elastic bending.
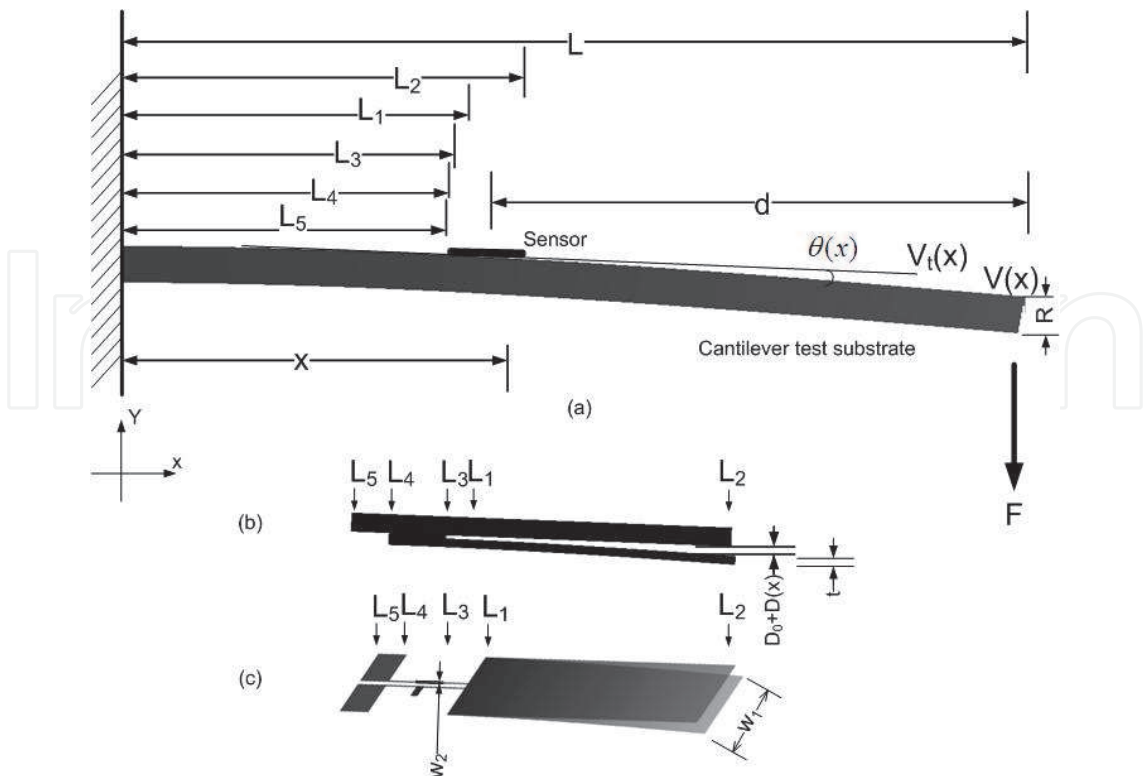
Fig. 2. The sensor on a substrate bar under bending. (b) The sensor's gap $D_0+D(x)$, zoomed in from above, varies as a function of position x. (c) shows the respect metal coordinates on the cantilever substrate.

The capacitance from two parallel electrode plates is given by

$$C = \varepsilon_0 \varepsilon_r \frac{A}{D} \tag{1}$$

where A is the area, D is the distance between two parallel plates, ε_0 is the permittivity and ε_r is the dielectric constant of the material between the plates. In order to measure the strain magnitude, a cantilever test substrate is utilized. For strain and capacitance calculations, it is assumed that the dimensions of the cantilever test substrate very large compared to the sensor and that the sensor is firmly affixed to the substrate. For a cantilever beam, the moment of inertia, I, is given by

$$I = \frac{WT^3}{12} \tag{2}$$

where, W is the beam width and T (or R as shown in Fig. 1) is the beam thickness. For a beam in uniaxial state of stress, the strain at any point on any surface under bending is given by a textbook (Hibbleer, 1997),

$$\varepsilon = \frac{\sigma}{E} = \frac{Mc}{EI} = \frac{6Fd}{EWT^2} \tag{3}$$

where σ is the stress on the surface, E is the Young's modulus of the steel bar substrate, M is the bending moment, c is the distance from the neutral axis to the surface, F is the force

applied at the free end of the beam and *d* is the sensor location from the free end of the beam. The sensor location on the beam is given by

$$d = L - \frac{L_4 + L_2}{2} \qquad (4)$$

where L is the length of the cantilever substrate, L_4 and L_2 are the longitudinal boundaries that define the bottom beam of the sensor. Fig. 2a shows the sensor location on the bent cantilever test substrate. Fig. 2b is the side view of a bending condition of the sensor design depicted in Fig. 2c, showing the sensor's metal layer coordinates and the widened gap, $D_0 + D(x)$. Figs. 2c also shows the details of the top and bottom electrode while under bending for the designs of interest. The initial sensor capacitance is given by

$$C_0 = \varepsilon_0 \varepsilon_r \frac{w_1(L_2 - M_1)}{D_0} + \varepsilon_0 \varepsilon_r \frac{w_2(M_1 - L_1)}{D_0} + C_p \qquad (5)$$

where L_1 marks the beginning of the metal layer on the bottom electrode, L_2 not only represents the boundary of the sensor but also the end of the metal layers on both the bottom and top electrode beams and therefore, $L_2 - L_1 = L_0$ is the effective electrode length. With various designs, M_1 is a variable that represents the start of the metal layer on the top electrode beam and also ends the trace that connects the electrode to the pad on the bottom beam. Therefore, $w_1(L_2 - M_1)$ represents the area of the overlapping metal plates, $w_2(M_1 - L_1)$ the area of the metal trace, and D_0 the initial spacing between the plates (see Figs. 2b-2c). The first term represents the capacitance of the overlapping metal plates. The second term is the capacitance of the trace between the electrode and the pad. The third term, C_p, is the parasitic capacitance of the metal traces between L_1 and L_3 combined with the planar pads between L_4 and L_5. L_3 is also the pivot point where the gap starts and L_5 is the physical boundary of the top electrode beam. Capacitance calculations for planar pads indicate that the third term is 0.035 pF (Baxter, 1997). In order to estimate sensor sensitivity to strain, the capacitance change caused by an applied strain is calculated using standard beam equations. The sensor metal plate attached to the beam will follow the beam deflection while the initially parallel plate will remain straight under deformation. The deflection of a cantilever beam and the attached sensor metal plate is given by (Hibbleer, 1997),

$$v(x) = \frac{-F}{6EI}(3Lx^2 - x^3) \qquad (6)$$

where the *v(x)*, as seen in Fig. 2a, is the vertical displacement at position *x* on the beam. The initially parallel plate remains straight and its position is represented by a line tangent to the deformed beam at the pivot point of the sensor. The tangent line (see Fig. 2a) is given by

$$v_t(x) = \theta(x)x + b \qquad (7)$$

where $\theta(x)$ is the slope at *x* and b is a constant determined by a boundary condition. The slope is determined from the first derivative of the deflection and given by

$$\theta(x) = \frac{-F}{2EI}(2Lx - x^2) \qquad (8)$$

At the sensor pivot point, L_3, from Fig. 4b, the deflection of the two metal plates is equal, providing the boundary condition

$$v_t(L_3) = v(L_3) \tag{9}$$

The constant b from (7) is solved by combining (6), (8) and (9) at point L_3 and becomes

$$b = \frac{F}{6EI}\left(3LL_3^2 - 2L_3^3\right) \tag{10}$$

Therefore, the tangent line is expressed as

$$v_t(x) = \frac{-F}{2EI}\left(2LL_3 - L_3^2\right)x + \frac{F}{6EI}\left(3LL_3^2 - 2L_3^3\right) \tag{11}$$

The increased gap (see Fig. 2b) between the two electrode plates is a function in the x-direction and expressed as

$$D(x) = v_t(x) - v(x) \tag{12}$$

The capacitance change is determined by calculating the average distance between the two metal plates of the strain sensor. The average displacement, in addition to the initial gap, between main metal layers is expressed as

$$D_1 = D_0 + \frac{1}{(L_2 - M_1)}\int_{M_1}^{L_2}(v_t(x) - v(x))dx \tag{13}$$

where M_1 is where the sensing portion of metal starts and L_2 where it ends. The capacitance due to the trace has an average displacement of D_2, which is expressed as

$$D_2 = D_0 + \frac{1}{(M_1 - L_1)}\int_{L_1}^{M_2}(v_t(x) - v(x))dx \tag{14}$$

where the metal stops at L_1. Capacitance, due to beam deformation, C_f, is given by

$$C_f = \varepsilon_0\varepsilon_r\frac{w_1(L_2 - M_1)}{D_0 + D_1} + \varepsilon_0\varepsilon_r\frac{w_2(M_1 - L_1)}{D_0 + D_2} + C_p \tag{15}$$

Combining (3), (13), (14) and (15), yields

$$C_f = \varepsilon_0\varepsilon_r\cfrac{w_1(L_2 - M_1)}{D_0 + \cfrac{\varepsilon(L(L_2^3 - M_1^3) - \frac{1}{4}(L_2^4 - M_1^4) + (3L_3^2L - 2L_3^3)(L_2 - M_1) + (\frac{3}{2}L_3^2 - 3L_3L)(L_2^2 - M_1^2))}{3dT(L_2 - M_1)}}$$

$$+ \varepsilon_0\varepsilon_r\cfrac{w_2(M_1 - L_1)}{D_0 + \cfrac{\varepsilon(L(M_1^3 - L_1^3) - \frac{1}{4}(M_1^4 - L_1^4) + (3L_3^2L - 2L_3^3)(M_1 - L_1) + (\frac{3}{2}L_3^2 - 3L_3L)(M1^2 - L_1^2))}{3dT(M_1 - L_1)}} + C_p \tag{16}$$

Based on the equation above, the bending strain sensor is analytically formulated and to be compared with the fabricated MEMS sensor in the following section.

2.2 Strain sensor fabrication

The sensor fabrication process is illustrated in Fig. 3. The materials include borosilicate glass (Pyrex Corning 7740, 500 µm thick) and silicon wafers (p-type, (100), 1-10 ohm-cm, double side polished, 310 µm thick). Fabrication began with clean glass and silicon substrates as shown in Figs. 3a and 3c. An electrode, traces, and a pair of contact pads were patterned onto the glass substrate by sputtering 0.02 µm chromium for adhesion layer followed by 0.2 µm of gold. The metal trace leading to the bonding area makes electrical contact with the silicon side electrode after anodic bonding. Wet etching was used to pattern the metal (Fig. 3b).The silicon wafer was wet oxidized (Fig. 3d), patterned using photolithography and etched with buffered oxide etch (BOE) solution to form an oxide mask for silicon surface machining. The wafer was etched using potassium hydroxide (KOH) at 85°C (approximately 0.7 µm / minute) to form recessed features and created the initial gap spacing. The etching mask was removed using BOE leaving two

Fig. 3. Cantilever bending strain sensor fabrication process. Illustrations on the left are the side views and on the right are the top views. (a) Pyrex (Coring 7400) glass, (b)sputter of Au/Cr on glass as one electrode, (c) silicon substrate, (d) oxidation of the silicon as the etching mask, (e) etching silicon with KOH to create platforms for anodic bonding with glass, (f) sputter Au/Cr on silicon as the other electrode, (g) side view of partial dicing (arrows marks) after glass and silicon are anodically bonded, (h) the individual sensor after final separation, noting the gap between the two electrodes.

silicon islands, which function as anchor platforms for the anodic bonding interface, as seen in Fig. 3e. An electrode and trace were then sputtered and patterned onto the silicon using the previously described metallization process. The small contact area on the raised anchor connected the pad on the glass plate with the electrode on the silicon plate via the traces, as seen in Fig. 3f.

The glass and silicon wafers were stacked with the metal surfaces facing each other and visually aligned using a mask aligner. Methanol was used to temporarily maintain alignment. The substrates were anodically bonded at 450 ºC on a grounded hotplate using a pointed probe to selectively place a -1000 V source on the glass, as shown in Fig. 3g. A gap is created between the electrodes on glass and silicon. This technique of selectively applying the electric field and bonding pressure prevented the recessed spaces from bonding to each other due to thermally induced warpage and electrostatic attraction. An automated dicing saw equipped with a 250 µm thick diamond blade was used to separate the individual sensor die from the bonded wafers. The silicon substrate was diced nearly through at the area above the contact pads. This was accomplished by limiting the depth of the cut and using the dicing alignment marks previously patterned on the silicon. Cuts to individually remove the sensors were similarly made from the silicon and glass substrate leaving approximately 30 µm of each substrate's depth (Fig. 3g). Care was taken to avoid chipping and prevent debris from filling the sensor gap. The sensors were separated from the wafer manually by flexing them to break the remaining thin substrate (Fig. 3h).

Sensors with less than 3 µm gap have been fabricated, but with unreliable capacitance values and low yield. It is because of the collapsing of the two electrodes during the anodic bonding process. In an effort to maintain high nominal capacitance, preserve sensitivity and promote linearity, a sensor with an electrode area of 2 mm x 4 mm, and a gap of 3 µm was fabricated for final SFMI prototyping. This sensor was tested on a spinal fusion rod with a near-linear response, as shown in Fig. 4.
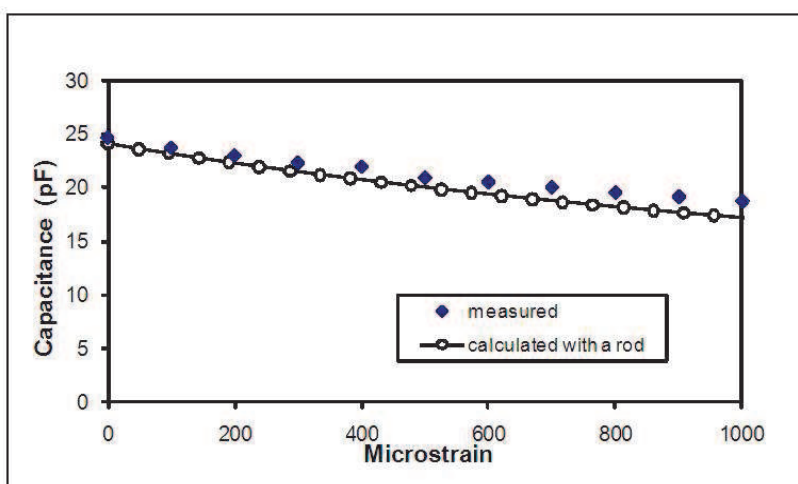

Fig. 4. Comparison of the calculation and experimental results of a strain sensor glued to a spinal fusion rod.

Gauge factor is defined as

$$GF = \frac{\frac{dC}{C}}{\varepsilon} \tag{2}$$

where dC/C is the fractional change of capacitance and ε is the strain. Using a linear fit of the differential capacitance data graphed in Fig 5, the gauge factor was ploted and calculated to be 252 for 0 to 1000 $\mu\varepsilon$. This value is extremly high in comparison to the current literature (Arshak 1994, 2000; Proctor & Strong 1992). By comparison, piezoresistive gauges typically provide a gauge factor less than 200 (Fraden, 1995) even at the cost of high temperature sensitivity.
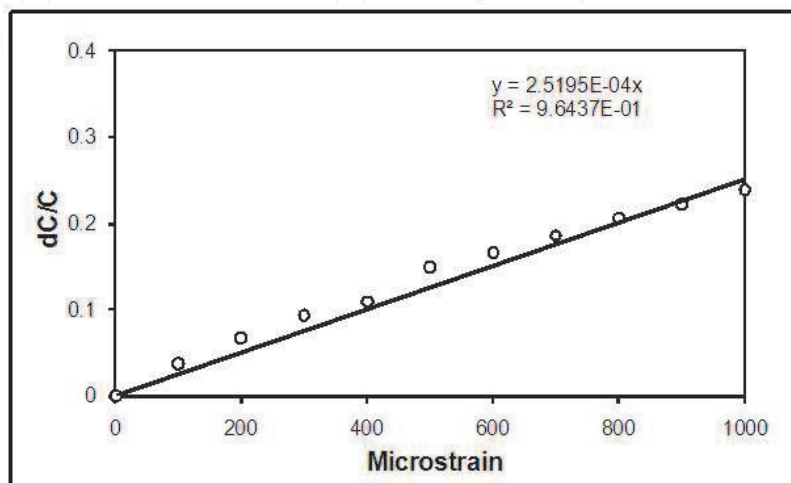

Fig. 5. Comparison of the calculation and experimental results of a strain sensor glued to a spinal fusion rod.

3. The transducer circuit

The transducer circuit is an inductively coupled, load modulated design similar in concept to Radio Frequency IDentification tags used for inventory and security. The 125 kHz magnetic field sourced by the interrogating reader induces a voltage in the LC tank of the implant. The LC tank (1 cm diameter, 600 turns) is resonant at 125 kHz. The AC voltage is then rectified, filtered, and regulated using a low quiescent power regulator. A supply of 3VDC, 28 μA is required to power the oscillator circuit described above and a frequency divider circuit composed of flip-flops. The oscillator frequency is divided to less than 1/20 the carrier frequency so that detection is simplified. The frequency divider also buffers the oscillator signal so that it can drive the gate of a MOSFET placed across the LC tank. The MOSFET acts a load that modulates the 125 kHz tank output at the divider output frequency. A diagram that shows the functionality can be seen in Fig. 6(a).

As it is functioned as an oscillator in Fig. 6(a), a capacitance to frequency (c-f) converter is used to convert the strain signal to a signal that can be transfered wirelessly. The c-f circuit is comprised of a pair of CMOS inverters (Lancaster, 1997) and can be seen in detail in Fig. 6(b). The oscillator produces a periodical voltage due to the charging and discharging of the RC across a threshold of an inverter input. The frequency of the RC oscillator is expressed as F=2.3R_tC, where C is the variable capacitor, or a capacitive strain sensor, and R_t is the matched resistance of the oscillator. The resistor R_I is to unload the RC network from clamping effect of protection diodes in the inverter. It will also result in a nearly square duty cycle and make the frequency less dependent of power supply variations. R_I is normally set about 10 times as higher as R_t to minimize the effect of the protection diodes. The oscillator oscillates empirically at 20 kHz with 20 pF capacitor and 100 kOhm resistor.
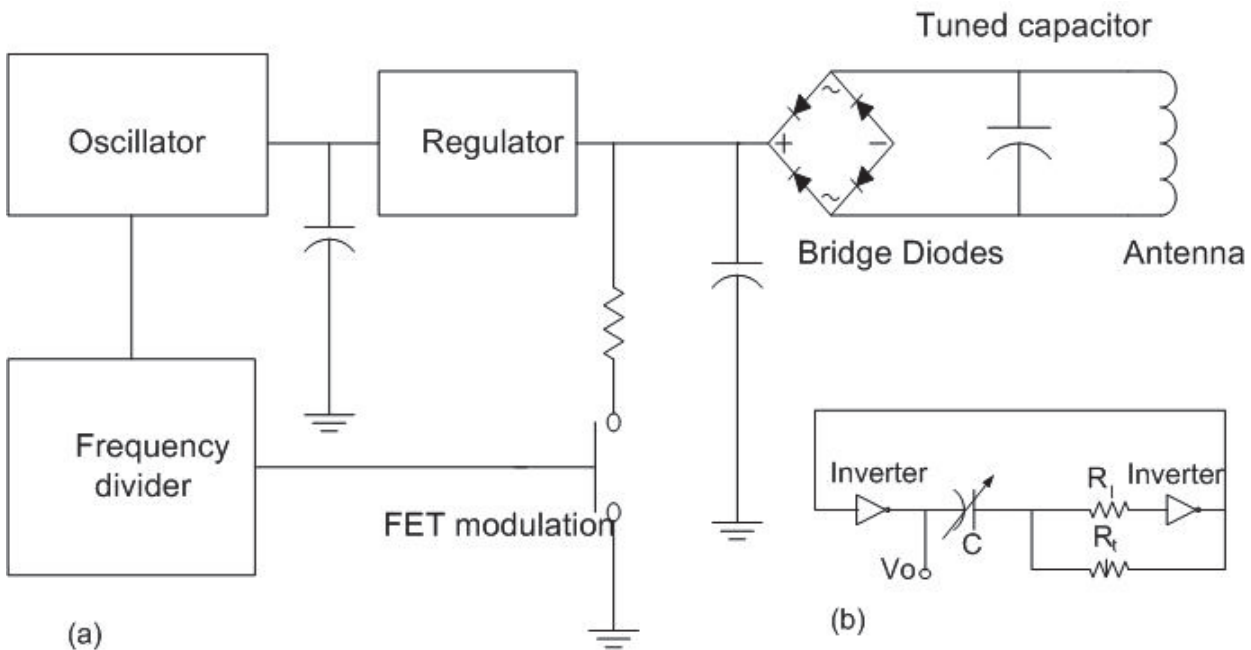
Fig. 6. The block diagram of the (a) transducer circuit and (b) oscillator circuit.

4. The interrogating reader

The interogating reader operating on 12 VDC, 175 mA provides the 125 kHz magnetic field for the implant, as illustrate in Fig. 7. The reader antenna is 24 cm in diameter and is tuned to 125 kHz. An EM Microelectronic (Marin, Switzerland), EM4095 IC contains an on-chip oscillator, antenna driver, and a demodulation circuit. The output of the demodulator is measured using an Agilent 53131A counter and logged with a computer based data acquisition system.

Fig. 7. The block diagram of the power reader.

4.1 Detection region

In the region of detection, see Fig. 8, the implant receives enough power to operate from the magnetic field sourced by the reader. There is no degradation of strain sensing performance

if sufficient DC power is available from the regulator. However at the far end of the region, planar and axial alignment becomes very important. With distance from the reader, inductive coupling is reduced thereby reducing the AC voltage across the LC tank and thus the modulated signal amplitude. The data signal also relies on the same low coupling between the implant and the reader. It is necessary to have a sensitive reader to detect the implant at the far end of the region.

Fig. 8. The detection region is within the cone shape.

5. The testing methods

The corpectomy model was used to evaluate the strain measurement system prior to spine testing. This model has similar bending to a four-point bending model therefore the rod strain does not change significantly along the length of the rod. A single metal foil strain gauge reference was attached to the rod adjacent to the housing for comparison to the transducer system. Comparing the metal foil reference gauge to the spinal fusion sensor placed in close proximity is justified. Figure 9 shows the sensor assembly on a housing without a container cover.

Fig. 9. The transducer sensor system on a housing that attaches to a stainless rod before a hermetically sealed container is assembled.

The strain measurement system was tested using a corpectomy model designed as a simplified mechanical analog of a spine section and then will be tested using a human spine. Figure 10 shows a free body diagram of the forces and bending moments applied to the spinal rods through the pedicle screws due to loading of the hard plastic blocks. Note that when the spinal fusion rods are fastened to the fixtures, often the initial strain is introduced and recalibrated. On the first test, the corpectomy apparatus was assembled inside a clear acrylic water tank without water on the MTS machine for application of the load; the sensor system was oriented facing out to be detected. The MTS machine's dynamic motion only changes 3 mm in the detection distance between the interrogating reader and the strain sensor. The read range was limited to 10 cm due to the reader design used and the sensor coil design constraints. A more optimal reader would increase the range. For other applications where a larger coil diameter is acceptable the range would be increased as well.

Fig. 10. The corpectomy model: front view, top and side view, bottom.

The data acquisition is obtained with LabView software, an interfacing program designed to transfer and record live data between instruments and computer by National Instrument. The strain information is recorded by the commecial metal foil strain gauge through a strain

indicator (Measurement group model P-3500). The frequency output from the wireless strain sensor system measurement is obtained through the digital universal counter (Agilent 53131A). In normal use, the response time for the strain indicator is 0.5 second, and the universal counter about 0.2 second. However, with the Labview interface the response time for the universal counter changes to 2.3 seconds but does not change for the strain indicator. The lag in time in the acquisition of the frequency data from the sensor system will cause false information when recording a drastic dynamic motion. In order to have a consistent and corresponding readings for the referred strain and the frequency output, a delay or pause in the live measurement is needed. Therefore, the MTS machine is programmed to pause 5 seconds at every increment of load for the frequency output to stabilize. Both the strain and the frequency data then are taken at the same time frame as the Material Test Machine.

The result of the telemetry strain sensor detection in Fig. 11 shows good linearity with R²= 0.99. The gauge factor is calculated to be 249 up to 1000 micro-strain, with R²=0.96 as see in Fig. 12. Similar gauge factor of 252 in the capacitance mode was measured in section 2. The frequency mode also exhibits high gauge factor without any amplification.
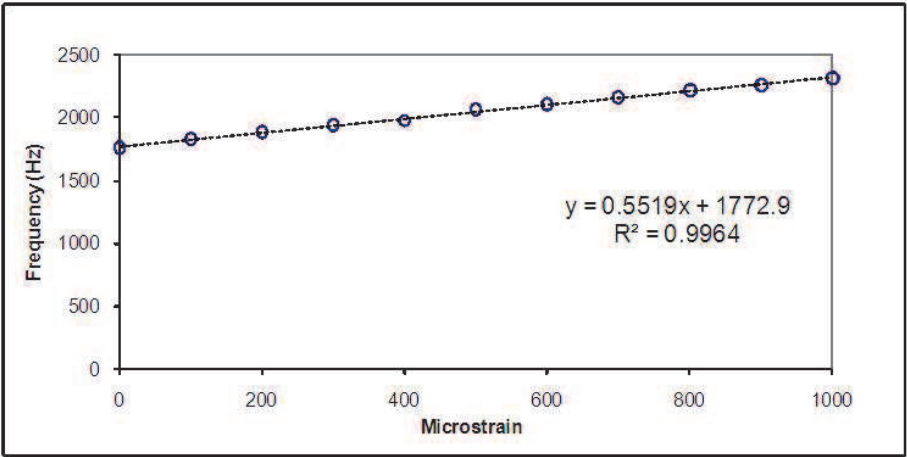

Fig. 11. The demodulate frequency responses from the sensor transducer shows a linear response due to bending test of the corpectomy model.
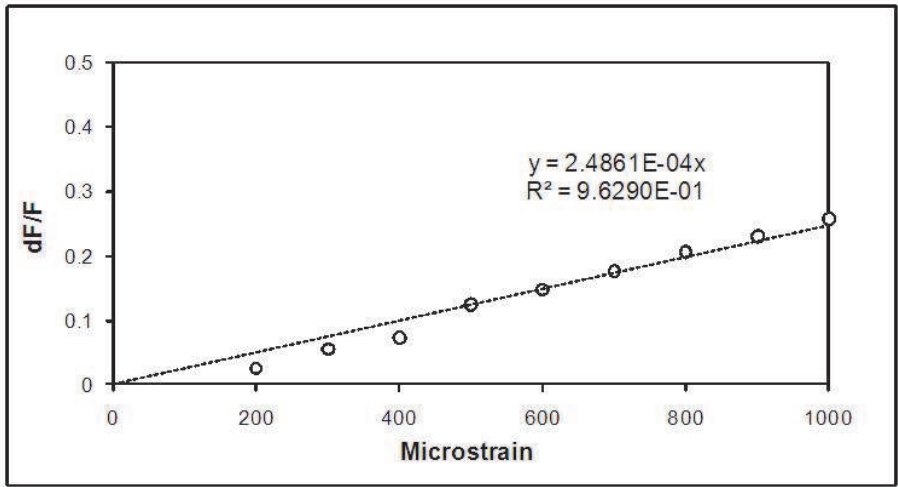

Fig. 12. The plot shows a linear gauge factor 249 in the frequency domain.

5.1 Water tank test

For the next application in water tank test, the sensor is expected to be in a fluidic environment. To protect from the influence of water or water vapor, the system was hermetically sealed in a container made of nylon and painted heavily with silicone and polyethylene. The container protected the device during corpectomy testing where it is submerged in a water tank used to simulate the body and during spine testing where it is in contact with tissue.

Caution has been taken for the temperature difference between water and ambient. A temperature dependent test on the sensor shows that the frequency drift from 1752 to 1778 Hz from 0 °C to 22.2 °C and vice versa with no strain at the rate of about 1.8 Hz/ °C. The interrgating reader was not moved at about 10 cm from the sensor system, through water, glass and air. The difference of the readings before the introduction of water and after was unnoticeable. The corpectomy model in water test was successful in showing the repeatability for the cyclic loads. It aslo suggests that measurements were possible in conditions present in-vivo. The tests of the corpectomy model in water tank were successful in showing that measurements were possible in conditions present in-vivo.

5.2 Excise spine test

A discectomy was performed on an excised spine from a cadaver and was constrained and loaded in a MTS system to simulate a 113.4 kg (250 lb) patient. The excised spine was potted using a liquid lead/bismuth alloy (Cerro Products, Bellefont, PA) and attached to a MTS Bionix mechanical testing system. A custom-built test apparatus was used to apply anatomic loads to the spine. The intact spine was tested by applying loads ranging from 100 to 200 N in an increasing and decrease manner with a 5-second period of pause at every increment to accommodate the detection speed of the system. The disc between L3 and L4 was surgically removed to simulate an unstable spine prior to fusion surgery, and the test sequence repeated. The comparison of results before and after the disk is removed are shown in Fig. 13.
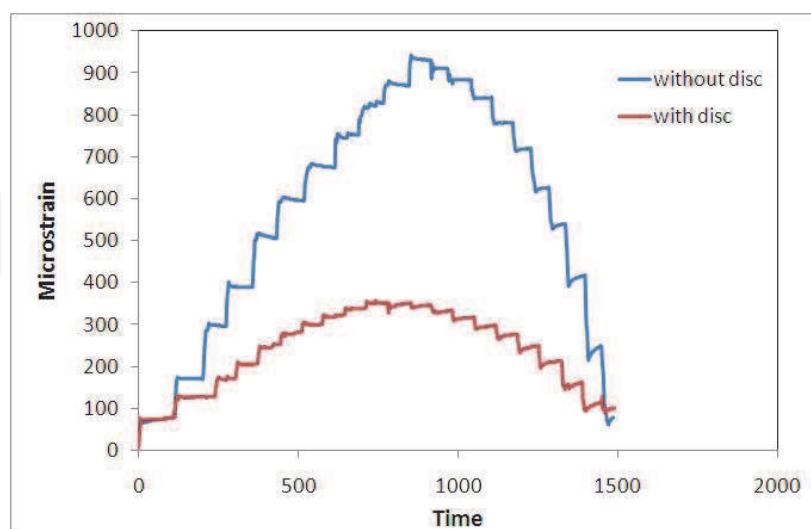

Fig. 13. Measured strains during excised spine testing.

With the same loading steps on the spine from MTS, the spinal fusion rods experienced less strain increment in the spine with the disk than that in the spine with the disk removed.

From the wireless transmision data along with the referred metal foil strain gauge, it is suggested that the spinal fusion rods showed that roughly one third of the load were shared by the intact spine after the spine is fused. The telemetry system clearly shows the rigidity of the intact spine.

6. Conclusion

A telemetry system using a capacitive strain sensor has been developed for the detection of spinal fusion monitoring. The strain sensor was made using MEMS process with high sensitivity and reduced size that serves the purpose for strain detection on the spinal fusion rod. The cantilever structure of the sensor is composed of two parallel plates, galss and silicon, respectively, with a narrow gap D_0 (3 μm) and a conjoint end. The bending strain sensor has the characteristics of high nominal capacitance (20 pF), high sensitivity, and compact dimensions (2 mm x 7 mm x 0.8 mm). It utilizes a variable gap configuration comprised of silicon and glass beams that are bonded at one end and open at the opposing end. This type of structure has been tested to withstand a strain range of 0 to 1000 με. The inductive link between the implant circuit and the reader was sufficient for supplying power to the implant circuit and extracting data at 10 cm distance. A specific sensor has a linear gauge factor of 252 in the capacitive domain and 249 in the frequency domain. Measurements made through air and water with a corpectomy model produced a linear response consistent with a metal foil reference gauge. The strain measurement system was also tested with the corpectomy model designed as a simplified mechanical analog of a spine section and was then tested using a human spine. For the biomechanics application, the sensor is expected to be in a fluidic environment. The tests of the corpectomy model placed in water tank were successful in showing that measurements were possible in conditions present in-vivo. The read range was limited to 10 cm due to the reader design used and the sensor coil design constraints. Finally, a test performed using a human spine showed the wireless implant detected strain roughly one third of the load were shared by the intact spine after the spine is fused.
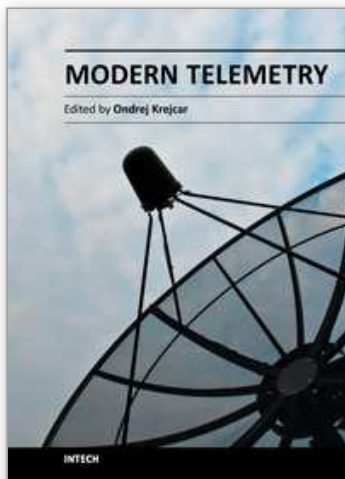
7. Acknowledgment

8. References

Aebersold, J.W.; Hnat, W.P.; Voor, M.J.; Puno, R.M.; Jackson, D.J.; Lin, J.T.; Walsh, K.M.& J.F. Naber (2007). Development of a strain transferring sensor housing for a lumber spinal fusion detection system, J. Med. Devices 1 (June 2007) 159-164.

Akar, O. ; Akin, T.& Najafi, K. (2001) A wire less batch sealed absolute capacitive pressure sensor, Sensor and Actuator A 95 (2001) 29-38.

Arshak, K.I.; Collins, D. & Ansari, F. (1994). New high gauge-factor thick-film transducer based on a capacitor configuration, Int. J. Electronics, 1994 vol. 77 No. 3, 387-399.

Arshak, K.I.; McDonagh, D. & Durcan, M.A. (2000). Development of new capacitive strain sensors based on thick film polymer and cement technologies, Sensors and Actuators A 79 (2000) 102-114.

Baxter, L. K. (1997). Capacitive Sensors: Design and applications, IEEE press, New York, 1997 pp 17-73

Benzel, E. & Ferrara, L. ; Roy, S. & Fleischman, A. (2002) Clinical Neurosurgery, 49, 209-225 (2002).

Chatzandroulis, S.; Tsoukalas, D., & NeuKomm P. A. (2000) A miniature pressure system with a capacitive sensor and a passive telemetry link for use in implantable applications, Journal of Microelectromechanicalsystems Vol.9 No.1 March 2000.

DeHennis, A.& Wise, K.D. (2002), A double-sided single-chip wireless pressure sensor, Digest IEEE conference on MEMS, (January 2002) Las Vegas. Pp 252-255. (2002) A Passive-Telemetry-Based pressure sensing system, Digest of the Solid-state Sensor and Actuator Workshop, (June 2002) Hilton Head,

DeHennis, A.& Wise, K.D. (2005). A wireless microsystem for the remote sensing of pressure, temperature, and relative humidity, J. of MEMS Vol. 14, NO. 1 February 2005 12-22.

Vamvanij, V.; Fredrickson, B.E.; Thorpe, J.M.; Stadnick, M.E.& Yuan, H.A. (1998). Surgical treatment of internal disc disruption: an outcome study of four fusion techniques, Journal of Spinal Disorders, Oct.11 (5) (1998) 375-382.

Finkenzeller, K. (1999). RFID Handbook: Radio-frequency identification fundamentals and applications, John Wiley & Sons, 1999 p 38.

Fraden, J. (1996) Hanbook of Modern Sensors (Springer-Verlag, New York, 1996)

Gibson, H. (2002). Measurement and finite element modeling of spinal rod strain, Master thesis, Dept of Mechanical Engineering University of Louisville, May 2002.

Harpster, T.J.; Hauvespre, S.; Dokmeci, M. R. & Najafi, K. (2002). A passive humidity monitoring system for in situ remote wireless testing of micropackages, J. of MEMS. Vol.11 No.1 February (2002) 61-67.

Hibbeler, R.C. (1997). Mechanics of Materials, Prentice Hall, New Jersey, 3rd ed., 1997 pp 584

Hnat, W.; Walsh, K. & Naber J. (2008). US Patent No 7357037.

Kanayama, M.; Cunningham, B.W.; Weis, J.C.; Parker, L.M.; Kanoda, K. & McAfee, P.C. (1997). Maturation of the posterolateral fusion and its effect on load-sharing of spinal instrumentation, Journal Bone and Joint Surgery Am. Vol. 79 (11) (1997) 1710-1720.

Lancaster, D. (1997). CMOS cookbook, Howard W. Sams & Co. Inc. pp 226.

Lin, J.-T.; (2006). Development of a telemetry spinal fusion sensor system, Ph.D. Dissertation, Electrical Engineering, University of Louisville, Louisville, KY.

Lin, J.-T.; Walsh, K. ; Jackson, D.; Aebersold, J.; Crain, M.; Naber, J. F. & Hnat, W. P. (2007). Development of capacitive pure bending strain sensor for wireless spinal fusion monitoring, Sens. Actuators,A,138 (2007) 276-28

Procter, E.& Strong, E. (1992) Capacitance strain gauges: strain gauge technology, Elsevier, 1992, PP 301-323.

Puers, R. (1993) Capacitive Sensor: When and how to use them, Sensors and Actuators A 37-38 (1993) 93-105.

Strong, Z.A.; Wang, A.W. & C.F. Mcconagh (2002). Hydrogel-actuated capacitive transducer for wireless biosensors, Biomed. Microdev. 4:2, (2002) 97-103.

Suster, M.; Chaimanonart,; N.; Guo,J.; Ko, W. H. & Young, D. J. (January 2005). Remote-Powered high-performance strain sensing microsystem, Technical Digest, the 18th IEEE International Conference on Micro Electro Mechanical Systems, Miami, Florida, January 2005, pp.255-258.

Modern Telemetry

Edited by Dr. Ondrej Krejcar

ISBN 978-953-307-415-3

Hard cover, 470 pages

Publisher InTech

Published online 05, October, 2011

Published in print edition October, 2011

Telemetry is based on knowledge of various disciplines like Electronics, Measurement, Control and Communication along with their combination. This fact leads to a need of studying and understanding of these principles before the usage of Telemetry on selected problem solving. Spending time is however many times returned in form of obtained data or knowledge which telemetry system can provide. Usage of telemetry can be found in many areas from military through biomedical to real medical applications. Modern way to create a wireless sensors remotely connected to central system with artificial intelligence provide many new, sometimes unusual ways to get a knowledge about remote objects behaviour. This book is intended to present some new up to date accesses to telemetry problems solving by use of new sensors conceptions, new wireless transfer or communication techniques, data collection or processing techniques as well as several real use case scenarios describing model examples. Most of book chapters deals with many real cases of telemetry issues which can be used as a cookbooks for your own telemetry related problems.

INTECH

open science | open minds